

# Characterization of Three *mnp* Genes of *Fomitiporia mediterranea* and Report of Additional Class II Peroxidases in the Order Hymenochaetales<sup>∇†</sup>

Ingo Morgenstern,\* Deborah L. Robertson, and David S. Hibbett

Clark University, Department of Biology, 950 Main Street, Worcester, Massachusetts 01610

Received 1 March 2010/Accepted 23 July 2010

**We report the sequence-based characterization and expression patterns of three manganese peroxidase genes from the white rot fungus and grape vine pathogen *Fomitiporia mediterranea* (Agaricomycotina, Hymenochaetales), termed *Fmmnp1*, *Fmmnp2*, and *Fmmnp3*. The predicted open reading frames (ORFs) are 1,516-, 1,351-, and 1,345-bp long and are interrupted by seven, four, and four introns, respectively. The deduced amino acid sequences encode manganese peroxidases (EC 1.11.1.13) containing 371, 369, and 371 residues, respectively, and are similar to the manganese peroxidases of the model white rot organism *Phanerochaete chrysosporium*. The expression of the genes is most likely differentially regulated, as revealed by real-time PCR analysis. Phylogenetic analysis reveals that other members of the order Hymenochaetales harbor *mnp* genes encoding proteins that are related only distantly to those of *F. mediterranea*. Furthermore, multiple partial *lip*- and *mnp*-like sequences obtained for *Pycnoporus cinnabarinus* (Agaricomycotina, Polyporales) suggest that lignin degradation by white rot taxa relies heavily on ligninolytic peroxidases and is not efficiently achieved by laccases only.**

Fungal class II peroxidases have been studied extensively since their discovery and initial characterization in the lignin-degrading model organism *Phanerochaete chrysosporium* (20, 65). They belong to the larger superfamily of non-animal peroxidases (47), originally described and termed the plant peroxidase superfamily by Welinder (67). The three-dimensional structure is strongly conserved among all known class II enzymes (2). Functional aspects of these enzymes have been studied in detail in *P. chrysosporium* (12, 37, 66). Fungal class II peroxidases can be divided into four groups based on the preferred substrates oxidized and the presence of key substrate-binding amino acid (aa) residues. Lignin peroxidases (LiPs) (EC 1.11.1.14) catalyze the oxidation of phenolic and nonphenolic aromatic compounds, such as synthetic lignins, by cleaving the C<sub>α</sub>-C<sub>β</sub> ether bonds but also act on the fungal metabolite veratryl alcohol (37). The reaction mechanism involves a long-range electron transfer pathway initiating from an exposed tryptophan residue (12, 48). Essentially the same pathway is present in versatile peroxidases (VPs) (EC 1.11.1.16), but additionally these enzymes contain three Mn-binding residues (9). Oxidation of Mn<sup>2+</sup> to Mn<sup>3+</sup> had been previously described as the major function of manganese peroxidases (MnPs) (EC 1.11.1.13), in which the same Mn-binding residues are present (18). Chelated Mn<sup>3+</sup> ions are thought to extract electrons from phenolic aromatic compounds directly or via lipid peroxidation from nonphenolic aromatics as well

(19, 40). There is significant evidence that the enzymes LiP, VP, and MnP act as ligninolytic enzymes, although some questions regarding the mechanism of lignin degradation still remain open (22). Functionally less well characterized is a fourth group of class II peroxidases represented by the *Coprinopsis cinerea* peroxidase (CiP) and the hybrid or novel peroxidase of *P. chrysosporium* (*nop* or *hip*). These enzymes are characterized as low-redox peroxidases and are considered to be non-ligninolytic (54).

Due to the potential biotechnological applications of ligninolytic peroxidases with respect to the improvement of feedstock quality for the production of second-generation biofuels, there has been an increased interest in the study of these secreted proteins. White rot fungi, which have the unique ability to degrade lignin, secrete these enzymes under ligninolytic conditions, which include nitrogen and carbon limitation (34, 60). Under laboratory conditions, heat shock, hydrogen peroxide concentration, oxygen supplementation, and growth medium characteristics (solid versus liquid, agitated versus stationary) influence the level of enzyme production (8, 17, 33, 53). MnP production depends on sufficient levels of Mn<sup>2+</sup> in the medium (7).

Much progress has been achieved in recent years regarding the evolution of the fungal peroxidase family, partly due to genome projects but also due to continued research interest in this family in non-model organisms. Phylogenetic analyses revealed that VPs arose independently at least twice, that LiPs are monophyletic and are presently known only from the Polyporales, and that MnPs are the most widespread ligninolytic peroxidases (41, 55). From an evolutionary perspective, two types of MnP can be distinguished. One type gave rise to LiPs and VPs, sharing a high degree of overall similarity with them, as is evident in protein length (354 to 365 residues; average, 363), exon-intron pattern (5 to 16 introns; median = 11), and the

\* Corresponding author. Present address: Centre for Structural and Functional Genomics (CSFG), Concordia University, 7141 Rue de Sherbrooke Ouest, Montreal, Quebec H4B 1R6, Canada. Phone: (514) 848-2424, ext. 8654. Fax: (514) 848-4504. E-mail: imorgenstern@gene.concordia.ca.

† Supplemental material for this article may be found at <http://aem.asm.org/>.

<sup>∇</sup> Published ahead of print on 30 July 2010.

number of disulfide bonds (four cystines). The second type of MnP is longer (376 to 395 aa; average = 383), has fewer introns (6 to 13; median = 6), and is characterized by an additional disulfide bond, presumably to stabilize the longer C terminus (62). Members of these "classical" or long MnPs form a monophyletic group that branches off early from the phylogenetic tree and contains a putative MnP sequence from *Fomitiporia mediterranea*, a member of the Hymenochaetales, in addition to sequences from the Polyporales and Corticiales (41). So far, sequences for MnPs, LiPs, and VPs have been detected only in wood-degrading white rot taxa, with the exception of an MnP from *Agaricus bisporus*, which is a leaf litter- and compost-degrading saprotroph. Class II peroxidases of yet unknown function are present in some brown rot taxa (25, 36) and in a diversity of ectomycorrhizal (ECM) taxa (4, 35).

In contrast to the Polyporales and Agaricales, other fungal taxonomic groups containing white rot taxa have been less well studied with respect to their ligninolytic peroxidase systems. The Hymenochaetales are a major order of the Agaricomycotina situated in a more basal position than the Polyporales and Agaricales (23). Members of this clade are almost exclusively wood-decaying white rot fungi and confirmed brown rot fungi are not present, but a few cases of ectomycorrhizal symbionts have been reported (31). Decay activity is usually described as mostly saprotrophic, but some species, notably *Porodaedalea pini* and *Phellinus igniarius*, qualify as timber pathogens (31). Two *Phellinus* species demonstrably decolorize textile dyes, a trait commonly attributed to phenoloxidase activity, but the actual enzymes involved have not been identified (1, 45).

*F. mediterranea* is a member of the Hymenochaetales that has an Old World distribution, where it occurs mainly on *Vitis vinifera* (16) and a few other host plants (14, 15, 63). The association between *F. mediterranea* and *V. vinifera* is of particular relevance, since the fungus produces an extensive white rot in the trunks of growing *Vitis* plants, which is one symptom of the destructive grapevine disease complex esca, affecting vine cultivation on a global scale (51). It is not yet clear if *F. mediterranea* acts independently from other pathogens or if the observed white rot decay is the result of favorable conditions created by a primary infection with ascomycetes (42). Surprisingly, expression of MnP and LiP in connection with the esca disease has been attributed to *Phaeoacremonium aleophilum* (anamorph of *Togninia minima*) (11, 43), and an MnP-like peroxidase was reported for *Phaeoacremonium viticola* and *Phaeoacremonium angustius* (46).

The purpose of our study was to determine if species in the Hymenochaetales have a reservoir of ligninolytic class II peroxidases that is comparable to enzymes characterized in the Polyporales or Agaricales. To achieve this we obtained additional partial peroxidase sequences for *F. mediterranea* and new sequences for other members of the Hymenochaetales. A further goal was to obtain the full-length sequences for *F. mediterranea* class II peroxidase genes and characterize them in a comparative way with the sequences from other lignin-degrading taxa. Finally, we monitored mRNA transcript abundance for *mnp* genes from *F. mediterranea* grown in liquid culture supplemented with different manganese concentrations.

## MATERIALS AND METHODS

**Strain and culture conditions.** A single spore isolate from *F. mediterranea* strain MF 3/22 was maintained on malt extract (ME) medium (2% malt extract, 2% agar, 0.05% yeast extract) in petri dishes and regularly subcultivated. Prior to DNA extractions, ca. 0.5-cm by 0.5-cm mycelium plaques from the mycelial growth zone on the surfaces of the agar plates were removed aseptically and transferred into 500-ml Erlenmeyer flasks containing 100 ml liquid ME medium (2% malt extract, 0.05% yeast extract). For RNA extractions, cultures were treated similarly but inocula were transferred into six-well Falcon plates (Becton Dickinson Labware, Franklin Lakes, NJ) containing 7.5 ml liquid ME medium per well. Cultures were grown without agitation under ambient conditions. When the cultures in the well plates covered approximately 80% of the surface area, the full nutrient medium was removed and the cultures were washed by being rinsed three times with distilled water, and after removal of excess liquid, 5 ml of the assigned experimental minimum salts medium was added to the cultures. Basal minimum salts medium contained the following per liter of distilled water: 0.2 g  $\text{KH}_2\text{PO}_4$ , 0.05 g  $\text{MgSO}_4 \cdot 7 \text{H}_2\text{O}$ , 0.01 g  $\text{CaCl}_2$ , 10 g glucose (56 mM) as a carbon source; 2.9 g ammonium tartrate (1.2 mM N) as a nitrogen source; 2.92 g sodium-2,2-dimethylsuccinate buffer (20 mM), pH 4.5; 1 ml mineral solution; and 1 ml vitamin solution (ICN Pharmaceuticals) (30). Mineral solutions were essentially the same as those described in reference 30 but were prepared separately for each experimental condition (zero/low/high Mn levels), differing only in the amount of  $\text{MnSO}_4 \cdot \text{H}_2\text{O}$  added. The final Mn concentration in the growth medium was 60  $\mu\text{M}$  for the high-Mn concentration treatment, 6  $\mu\text{M}$  for the low-Mn concentration treatment, and 0  $\mu\text{M}$  for manganese-free treatment.

**DNA and RNA extractions.** Genomic DNA from *F. mediterranea* cultures was extracted from 3 to 5 g fresh material after vacuum filtration using a maxi-prep protocol (<http://www.clarku.edu/faculty/dhibbett/protocols.html>) and purified with the GeneClean II kit (Bio 101, La Jolla, CA), quantified spectrophotometrically, and stored at  $-20^\circ\text{C}$ . On days 1, 3, 5, and 7 after medium exchange, RNA was extracted from 90 mg fresh material after vacuum filtration using the Qiagen RNeasy mini kit (Valencia, CA) and mechanical disruption using a Mini-Bead-beater-8 (BioSpec Products, Bartlesville, OK). Mycelia were homogenized by twice disrupting the cells for 4 min each and interrupted by cooling the material on ice for a few minutes. Purified RNA was stored at  $-80^\circ\text{C}$ .

**Standard PCR and sequencing analyses.** Newly generated partial sequences for this study were obtained as previously described using primer combinations aVP-1F/BLP-7R and hymMP-f/hymMP-r (41). We focused on members of the Hymenochaetales but included also members of the Polyporales. Thermal cycle parameters were as follows: a 2-min initial denaturation at  $95^\circ\text{C}$ , 30 cycles of 30-s denaturation at  $94^\circ\text{C}$ , 30 s of annealing at  $55^\circ\text{C}$ , a 1-min extension at  $72^\circ\text{C}$ , and a 10-min final extension at  $72^\circ\text{C}$ . Purification and molecular cloning of amplification products was done as described in a previous study (41). Sequencing was carried out on an ABI Prism 3130 genetic analyzer (Applied Biosystems, Foster City, CA).

**IPCR analysis.** Genomic DNA was digested with the restriction enzymes *Mse*I, *Nsp*I, *Apo*I, and *Hind*III (New England Biolabs). Restriction digests were carried out with 2.0 to 3.0  $\mu\text{g}$  total genomic DNA for 3 h at optimum temperatures ( $37^\circ\text{C}$  for *Mse*I, *Nsp*I, and *Hind*III and  $50^\circ\text{C}$  for *Apo*I) in 50- $\mu\text{l}$  reaction volumes and 20 U of restriction enzyme per reaction mixture. After purification (Qiagen), digested DNA was diluted 5-fold and ligated in a 50- $\mu\text{l}$  reaction volume using 40 U of T4 DNA ligase (New England Biolabs) at  $16^\circ\text{C}$  for 16 h. For each sample DNA, three ligation reactions were carried out with increasing amounts of template (5  $\mu\text{l}$ , 10  $\mu\text{l}$ , 25  $\mu\text{l}$ ). First-round inverse PCR (IPCR) was carried out using 5- $\mu\text{l}$  aliquots from the ligation reaction, 12.5 pM of each inner IPCR primer (Table 1), 0.2 mM each deoxynucleoside triphosphate (dNTP), 2.5  $\mu\text{l}$   $10\times$  reaction buffer, and 1.25 units *Taq* DNA polymerase in a 25- $\mu\text{l}$  reaction volume. First-round PCR conditions were as follows: initial denaturation at  $95^\circ\text{C}$  for 2 min, followed by 9 cycles of denaturation at  $94^\circ\text{C}$ , annealing in a touchdown approach starting at  $60^\circ\text{C}$  and ending at  $52^\circ\text{C}$  ( $-1^\circ\text{C}$  per cycle) for 40 s, and extension at  $72^\circ\text{C}$  for 2 min 15 s, followed by 37 cycles of denaturation at  $94^\circ\text{C}$  for 45 s, annealing at  $52^\circ\text{C}$  for 1 min 30 s, and extension at  $72^\circ\text{C}$  for 2 min 15 s, followed by a final extension at  $72^\circ\text{C}$  for 15 min. Amplification products were column cleaned (Qiagen) and subjected to second-round PCR analysis with nested outer inverse PCR primers. A 5- $\mu\text{l}$  aliquot from the first-round PCR was used as a template in the second-round PCR in a total reaction volume of 25  $\mu\text{l}$ . Second-round amplification parameters consisted of initial denaturation at  $94^\circ\text{C}$  for 2 min, followed by 35 cycles at  $94^\circ\text{C}$  for 30 s,  $53^\circ\text{C}$  for 30 s, and  $72^\circ\text{C}$  for 1 min 15 s, followed by a final extension at  $72^\circ\text{C}$  for 10 min. Amplification results were visualized with ethidium bromide staining of a 1% agarose gel after gel electrophoresis of an aliquot. Reaction results producing a single band were purified (Qiagen) and cloned using the TOPO TA cloning kit (Invitrogen).

TABLE 1. Primers used in this study

Primer	Sequence (5'→3')	Application
aVP-1F	TGC GGC GAA GAW GTR CAC G	Standard PCR
bLP-7R	MCG AAS GAY TGC CAY TCR CA	Standard PCR
hymMP-f	GAR TCY CTS CGC MTS ACB TTC C	Standard PCR
hymMP-r	GTT GAC GAW GGM TTG CCA KWM RCA	Standard PCR
Fmed_MP_1141	GCA TGA TCG AGC CAT CGG	Inverse PCR, outer
Fmed_MP_1426	CTC GAG TTG AGG TGC TCC	Inverse PCR, inner
Fmed_MP_r484	CCA CAA GAC CCT GTT GGC	Inverse PCR, inner
Fmed_MP_r713	GTG CAG AAG TTC TGT CGC C	Inverse PCR, outer
Fmed_MP_r1590	GTG TTG AAG TCG CGG TGC	Inverse PCR, outer2
Fmed1V_187	GAG GCT GGC GCA AAG TGG AAG ATC	Inverse PCR, outer
Fmed1V_1200	TTG GCT GGA TCA GCG AGT TCG GTG	Inverse PCR, inner
Fmed1V_r531	TAC TCC CTT CAC GTT CGA CCC GC	Inverse PCR, inner
Fmed1V_r632	TCG ACT CAC CGC TTC CTC AGT CTG	Inverse PCR, outer
Fmed9V_1141	GCC CGC GAA CTG TCC TGT TAA CG	Inverse PCR, outer
Fmed9V_1231	AAG GGC ATC AGT GCC ATC CTC AG	Inverse PCR, inner
Fmed9V_r605	TGG AGC CGA ACA TTA CTG GTG GTG	Inverse PCR, inner
Fmed9V_r688	GCT CGC GAT TTC GTA CGT CAC TGC	Inverse PCR, outer
Fmed3_1170	GCT AGA CAT TCT GGT GAC CCG AGG	Inverse PCR, outer2
Fmed3_1521	CTG CAA GAG CGA CGA CAG TCG	Inverse PCR, inner2
Fm_EF1a_RTf	TGG ATT GCC ACA CTG CCC ATA TTG	Real-time PCR
Fm_EF1a_RTr	GGT TTG CCT CAT GTC ACG CAC	Real-time PCR
Fm_mnp1_RTf	ACG GCA TTC CAA ACG TCC ATG AAG	Real-time PCR
Fm_mnp1_RTr	GCA CCA GGG TCC GTA GAA AGA GTA	Real-time PCR
Fm_mnp2_RTf	GGC AAT CAA TGG TTG CAA ACC AGC	Real-time PCR
Fm_mnp2_RTr	AAT CTG AGT CGG TTF TCC ACC G	Real-time PCR
Fm_mnp3_RTf	CGT CTT CAA TCT GAC TTC GCC CTC	Real-time PCR
Fm_mnp3_RTr	GAG ATC GGA GCA GTC AAC GAG C	Real-time PCR

**RT-PCR and real-time PCR analyses.** Transcript levels of the three newly characterized *mnp* genes in *F. mediterranea* were measured in comparison to the transcript levels of the housekeeping gene *ef-1 $\alpha$*  and are interpreted as relative expression levels. First-strand cDNA was synthesized from 0.1  $\mu$ g total RNA using the QuantiTect reverse transcription (RT) kit (Qiagen) according to the manufacturer's guidelines. Genomic DNA was eliminated from the samples by incubation of samples for 4 min at 42°C with the supplied genomic DNA (gDNA) wipeout buffer prior to reverse transcription. For control purposes, each sample was also reverse transcribed without reverse transcriptase added to the master mix. Second-strand cDNA generation was obtained by using real-time PCR analysis on a Stratagene Mx3000P thermal cycler. Real-time experiments were conducted in triplicate from each biological sample using the Brilliant II SYBR green quantitative PCR (qPCR) master mix (Stratagene) with final primer concentrations of 0.2  $\mu$ M (*ef-1 $\alpha$* -specific primers) and 0.3  $\mu$ M (all *mnp*-specific primers) per reaction. Amplification conditions were as follows: 10 min at 95°C, 40 cycles of 30 s at 95°C, and 1 min at 60°C, followed by a final dissociation cycle with 1 min at 95°C, 30 s at 55°C, and a ramp phase of up to 95°C with a 0.2°C increase per second. The mean normalized expression was calculated using the Q-Gene module (<http://www.gene-quantification.de/download.html>) by averaging the three threshold cycle ( $C_T$ ) values of each replicate and subsequent calculation of the mean normalized expression (44). Accordingly, the standard error was calculated using the differential equation of Gauss for error propagation. The amplified products were run in 1.6% agarose gels for size comparison, purified, cloned as described above, and sequenced to verify specificity of the amplicons obtained from qRT-PCR.

**Phylogenetic analyses.** The three full-length *mnp* sequences from *F. mediterranea* and 22 partial class II peroxidase sequences generated by this study were added to a preexisting data set (41). We amplified partial sequences for *Phylloporia ribis*, *Inonotus hispidus*, *Hymenochaete corrugata* (Hymenochaetales), *Pycnoporus cinnabarinus*, *Grifola frondosa*, and *Steccherinum fimbriatum* (Polyporales). Previously, no class II sequences were available for any of these white rot taxa. An additional 16 class II peroxidase sequences, mostly from ectomycorrhizal taxa but also including some from the white rot fungus *Phellinidium ferrugineofuscum* (Hymenochaetales), were obtained from a recent study (4). BLASTP searches against the NCBI GenBank detected 21 more sequences. After pruning redundant sequences, the final data set contained 177 sequences (77 full length and 100 partial). Multiple sequence alignment was performed with MAFFT using the E-INS-i setting (28, 29). The signal sequence and one ambiguous region present only in the two outgroup sequences were excluded from the

analyses. Bayesian analysis was run for 10 million generations with eight Markov chain Monte Carlo (MCMC) chains in two runs, each with 1 cold and 3 heated chains for 10 million generations, mixed model for amino acid substitutions, and trees sampled every 1,000 generations using MrBayes v3.1.2 (26, 52). Convergence of likelihood scores was established with Tracer v1.4 (<http://beast.bio.ed.ac.uk/Tracer>), and the first 3,000 trees from each run were removed as the burn-in before calculating the consensus tree. Maximum likelihood (ML) analyses were performed using RAXML (59) with the rapid hill-climbing algorithm and the WAG substitution model. A tree with the best likelihood scores was obtained from an analysis combining the search for the best ML tree with the rapid bootstrap analysis using 100 bootstrap replicates, and final bootstrap support was estimated from a run with 1,000 bootstrap replicates.

## RESULTS

**Characterization of three *F. mediterranea mnp* genes.** Using standard and inverse PCR analyses, we obtained the full-length sequences of three putative *mnp* genes from *F. mediterranea*. Putative intron-exon boundaries as well as start and stop codons were predicted based on homologous sequences. The leader sequence was identified using SignalP 3.0 (3). Accordingly, gene *Fmmp1* consists of a 1,516-bp open reading frame (ORF) interrupted by seven introns (see Fig. S1a in the supplemental material). The deduced amino acid sequence of the prepropeptide is 371 aa long and includes a 18-aa signal peptide, followed by a 5-aa propeptide leader sequence that ends with a KEX2 motif (Lys-Arg). The mature protein is predicted to contain 348 aa. *Fmmp2* (see Fig. S1b) has a 1,351-bp-long ORF and is interrupted by four introns. The amino acid sequence of the prepropeptide encoded by *Fmmp2* is 369 aa long, including a 17-aa-long signal peptide and 5 aa with the KEX2 motif preceding the mature peptide. The ORF of *Fmmp3* is 1,345 bp long (see Fig. S1c). The predicted coding sequence is interrupted by four introns. The prepropep-

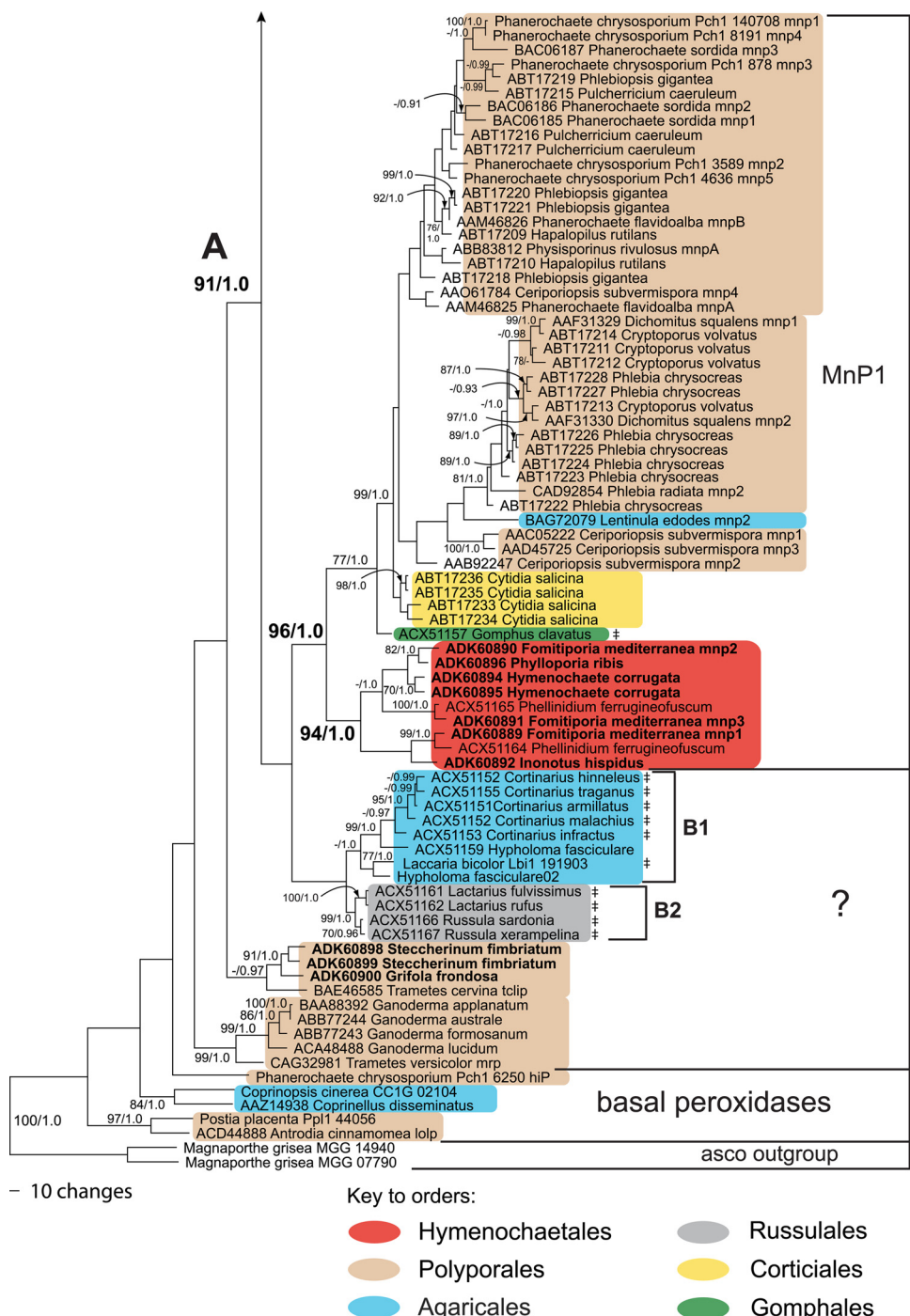


FIG. 1. Maximum likelihood tree showing phylogenetic relationships of class II fungal heme peroxidases. ML bootstrap support values above 70 are indicated before the slash. Bayesian posterior probability values above 0.9 are indicated after the slash. Fungal orders are distinguished by colored boxes. ‡, ectomycorrhizal taxa. Sequences generated by this study are in bold. Labeling of clades and clusters takes phylogenetic considerations and structural-functional aspects into account, which are based on the presence of crucial residues in the protein sequence. Accordingly, MnPs are characterized by the presence of the Mn-binding site (three acidic residues) and the absence of an exposed tryptophan. VPs are characterized by the presence of the Mn-binding site and the exposed tryptophan. LiPs are characterized by the presence of the tryptophan and the absence of the Mn-binding site. Some partial sequences do not cover all three Mn-binding residues and/or the exposed tryptophan.

tide sequence is 371 aa long and contains a 19-aa-long signal sequence and the 5-aa propeptide leader sequence. The presence of a KEX2 cleavage motif is common among most class II peroxidases, but it is not present in the long MnPs from the

Polyporales (Fig. 1, clade MnP1, without Hymenochaetales). MnPs from the Hymenochaetales seem to have retained this feature before it was lost in the lineage leading to the Polyporales. However, MnPs from *F. mediterranea* share with the long

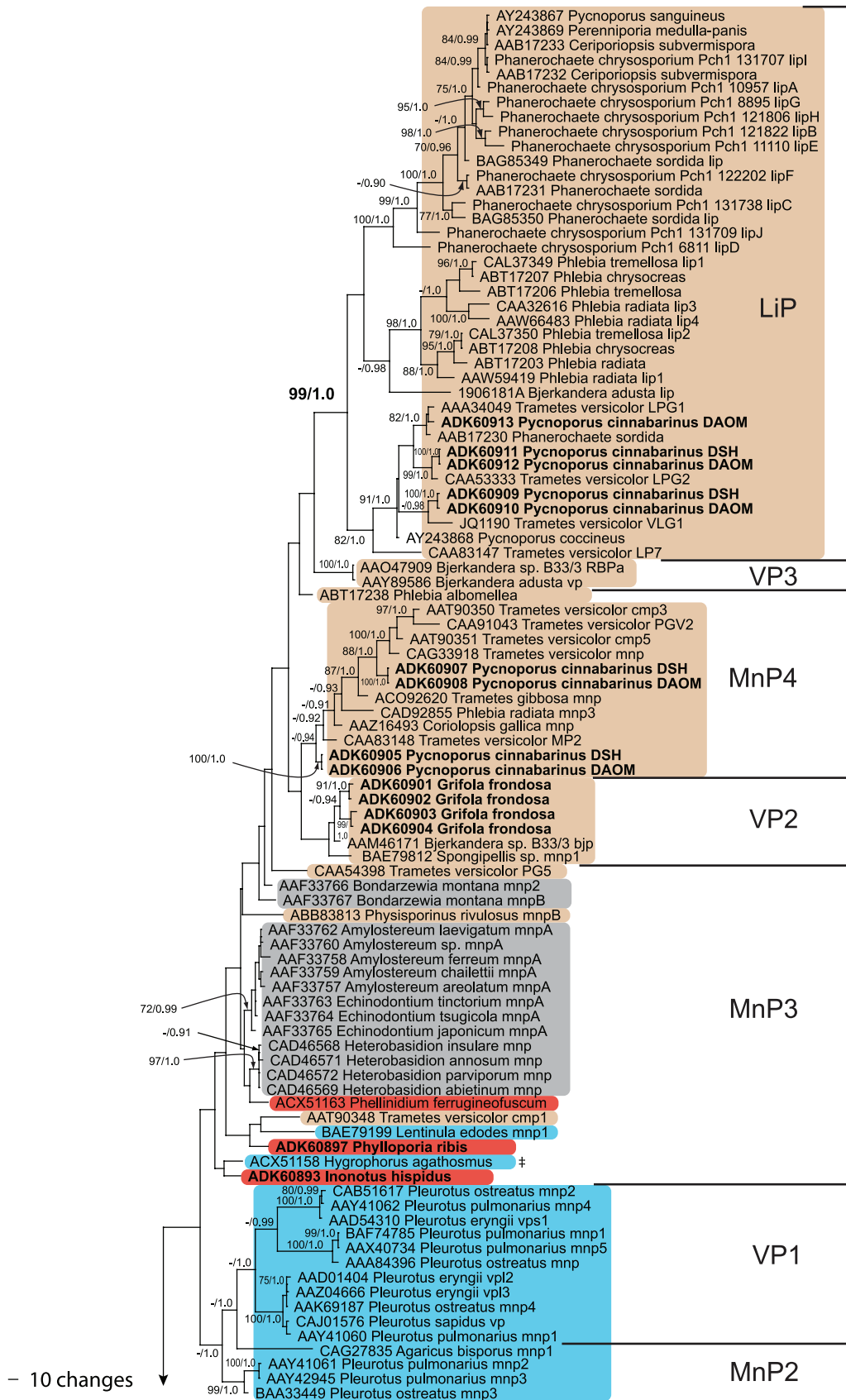


FIG. 1—Continued.

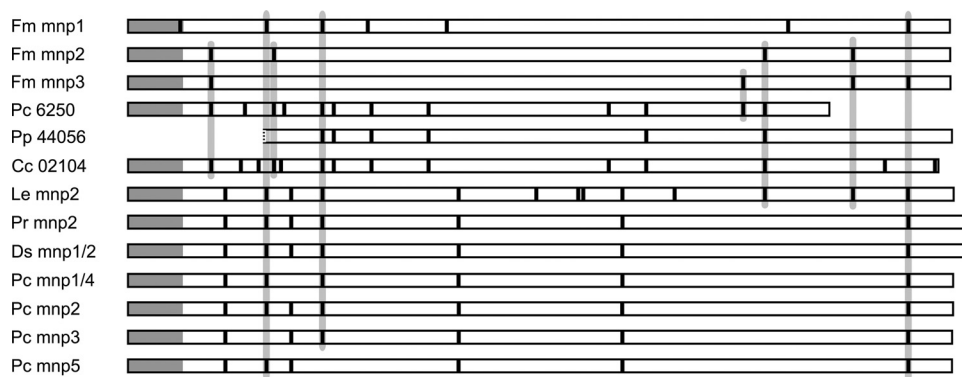


FIG. 2. Comparison of intron distribution for the three new *F. mediterranea* peroxidase genes with 10 selected full-length sequences from clade MnP1 and basal peroxidases. Introns are shown as black bars, signal peptides are shaded dark gray, and introns shared between *F. mediterranea* and other taxa are light gray. Cc, *Coprinopsis cinerea*; Ds, *Dichomitus squalens*; Fm, *Fomitiporia mediterranea*; Le, *Lentinus edodes*; Pc, *Phanerochaete chrysosporium*; Pp, *Postia placenta*; Pr, *Phlebia radiata*.

MnPs from *P. chrysosporium* and other Polyporales (Fig. 1, clade MnP1) two additional cysteine residues, allowing the formation of a fifth disulfide bond. These cysteine residues are 7 aa apart and their positions are well conserved. However, in *F. mediterranea* only isoform MnP1 cysteines occupy exactly the same positions; in isoforms MnP2 and MnP3, the distance between the cysteine residues is 9 aa. The stop codon in the *F. mediterranea* MnPs (FmMnPs) follows only three and four residues after the last cysteine, whereas other MnPs in clade MnP1 have between 9 to 21 residues before the stop codon, giving the mature protein a considerably longer C-terminal tail. Residues important for peroxidase function, which are conserved throughout the peroxidase superfamily, are present in the three *F. mediterranea* MnPs, and include the distal and proximal histidine and other residues involved in heme pocket formation. Mn-binding residues and putative N glycosylation sites (consensus sequence N-X-T/S) have been identified and are indicated (see Fig. S1a to c in the supplemental material). The calculated isoelectric points and molecular masses for the holoenzymes are as follows: pI 4.71, 39.3 kDa for FmMnP1; pI 4.25, 38.7 kDa for FmMnP2; and pI 4.52, 39.1 kDa for FmMnP3. *Fomitiporia mediterranea* MnPs lack the exposed tryptophan residue characteristic for LiPs and VPs; however, this position is uniquely occupied by a histidine residue in FmMnP2 and FmMnP3 and in other partial sequences from hymenochaetalean taxa. Predicted introns ranged in size from 51 to 63 nucleotides (mean, 58), and all followed the canonical GT-AG splice rule. In contrast to the *P. chrysosporium mnp* genes that have a remarkably conserved exon-intron pattern, none of the *F. mediterranea* introns is present in all three *mnp* genes. A comparison with other *mnp* genes and basal peroxidases reveals that the intron positions in *F. mediterranea* are more similar to those in basal peroxidases and *Lentinus edodes mnp2* than to those in *mnp* genes from the Polyporales (Fig. 2). We found several unique predicted introns in *Fmmnp1* that are not shared with any other peroxidase used in the comparison.

**Comparison of relative expression levels.** Quantitative RT-PCR experiments resulted in a single product for each primer pair evident from dissociation curve analyses as well as from cloning and sequencing of the obtained RT-PCR amplicons, confirming expression of the three putative *mnp* genes in *F.*

*mediterranea*. The transcript abundance for each isoform varied, depending mostly on the time after nutrient exchange and to a lesser degree on the manganese concentration in the medium. Manganese availability apparently did not influence the transcript level for any isoform on day 1 (Fig. 3). Transcript levels for isoforms *Fmmnp1* and *Fmmnp2* displayed a similar overall pattern, which differed from *Fmmnp3* levels. Transcripts of the two former isoforms increased over the time course of the experiment, peaking on day 5 in the high-manganese concentration medium, whereas *Fmmnp3* levels decreased, without apparent influence by manganese concentration (Fig. 3). Isoform *mnp2* transcripts were expressed at levels approximately 2-fold higher than *mnp1* transcripts under any experimental treatment. On the last day of the experiment (day 7), elevated manganese levels led to decreased expression of isoforms *mnp1* and *mnp2*, and the highest expression was recorded in the manganese-free medium.

**Phylogenetic placement of the Hymenochaetales class II peroxidases.** The final data set containing 177 sequences from 70 species includes 77 full-length and 100 partial sequences (see Table S1 in the supplemental material). The total length of the aligned sequences was 566 characters; 419 characters were included for phylogenetic analyses. Bayesian analysis and maximum likelihood analysis produced consensus trees with similar topologies, but results did not always agree regarding the placement of some groups lacking solid support from both analyses (results not shown). The tree shown in Fig. 2 depicts the tree with the best likelihood score ( $-29\,188.97 \ln$ ) from the ML analysis.

The phylogenetic analysis places the majority of Hymenochaetales sequences, including the three *F. mediterranea* MnPs and partial sequences from *Hymenochaete*, *Phylloporia*, and *Inonotus* species generated by this study, at the base of clade MnP1 (Fig. 1). This clade contains the long-MnP forms, characterized by their additional disulfide bond. The remaining three partial Hymenochaetales sequences are placed in the central part of the tree (MnP3) that not only lacks support values on backbone nodes, but in this part the branching order to the tips also remains completely unresolved. The Hymenochaetales sequences do not cluster together; instead, each

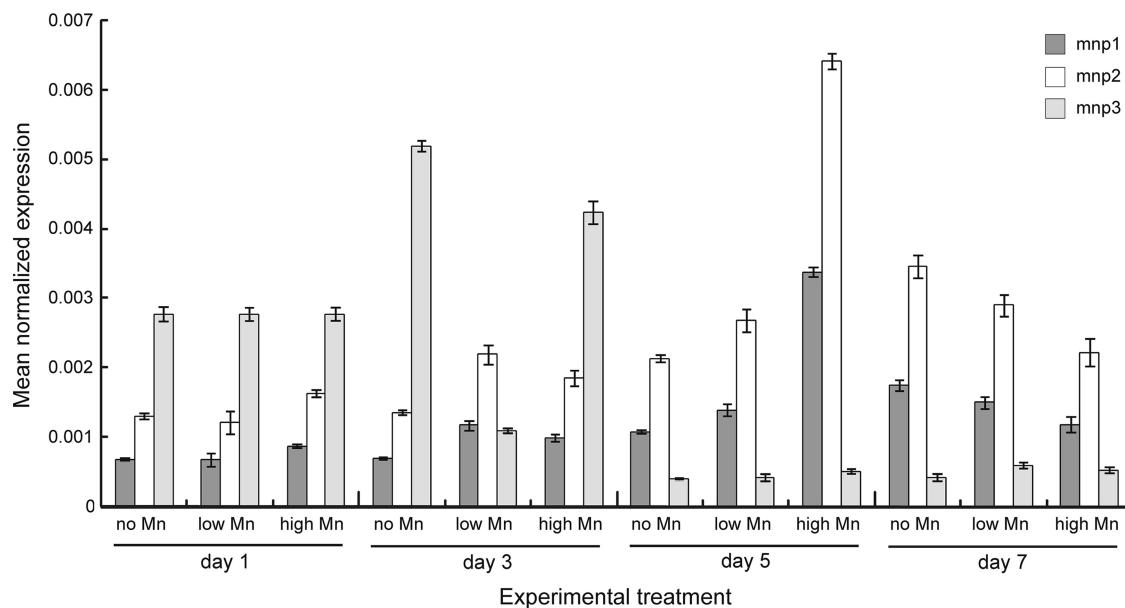


FIG. 3. Mean normalized expression (MNE) of *mnp1*, *mnp2*, and *mnp3* transcripts from *F. mediterranea* grown in Mn-free medium, low-Mn concentration medium, and high-Mn concentration medium for 1, 3, 5, and 7 days.

sequence seems to be more closely related to sequences from taxa belonging to other orders.

At the base of the tree, a small paraphyletic assemblage of basal peroxidases is placed next to the two outgroup sequences. If there is a common characteristic of this group, then it is that they seem to be monotypic; i.e., basal peroxidases do not appear in multiple isoforms. A second, albeit much larger, paraphyletic group labeled with a question mark (Fig. 1) contains sequences from white rot fungi from the Polyporales and mostly ectomycorrhizal fungi from the Agaricales and Russulales (64). The correct placement of these groups remains unresolved because the inner nodes in this part of the tree did not receive strong support values. Monophyly of all ectomycorrhizal sequences is not supported, but they are supported as members of a clade (Fig. 1, clade A) encompassing all ligninolytic peroxidases (MnP/LiP/VP). The function of the sequences in ectomycorrhizal taxa is unknown, and only limited functional data are available for the sequences from white rot taxa situated between the basal peroxidases and the core group (Fig. 1, clade A).

A large clade of MnPs (MnP1), in a sister relationship to the ectomycorrhizal sequences, receives solid support (96/1.0, bootstrap support [BS]/posterior probability [PP]) and harbors mostly sequences from the Polyporales and, branching off early, a clade (94/1.0, BS/PP) containing exclusively Hymenochaetales sequences. The central part of the tree is characterized by alternating clusters of sequences that can be attributed to MnPs and VPs. The support for these clusters is mixed. In the Agaricales, MnPs and VPs belonging to *Pleurotus* species are clearly separated, but an MnP from *Agaricus bisporus* seems to be more closely related to the VPs than to the MnPs of species of *Pleurotus*. The monophyly of the *Pleurotus* and *Agaricus* clade, as well as the functional separation (MnP2 and VP1), is supported only by the Bayesian analysis. A cluster containing the partial sequences from *Grifola frondosa*

is tentatively assigned to VPs (VP2). The only full-length sequence containing all aa residues characteristic for VPs belongs to *Spongipellis* sp., but the position receives no support from both analyses. However, the *Grifola* sequences also contain the residues (tryptophan, leucine) for LiP-type substrate interaction along with the third Mn-binding residue (aspartate), which is usually missing in peroxidases without a manganese-oxidizing capacity. Support values are better for the last MnP cluster (MnP4), which contains two sets of sequences from two different *Pycnoporus cinnabarinus* strains. This finding is the first evidence for *mnp* genes in *P. cinnabarinus*. No differences in aa composition between the two strains are observed. Clusters MnP4 and VP2 harbor only sequences from the Polyporales. Two sequences from *Bjerkandera* species constitute the third and smallest VP cluster. Due to the lack of statistical support, it remains unresolved if this is indeed a third origin of VPs, but these sequences do consistently group with LiPs in phylogenetic analyses. The last major clade receives strong support from both analyses (99/1.0, BS/PP) and contains LiPs from Polyporales, including sequences from *P. cinnabarinus* presented here for the first time. These sequences lack the Mn-binding residues, with the exception of *Trametes versicolor* LP7.

## DISCUSSION

The three *F. mediterranea* peroxidase sequences described here are the first characterized full-length sequences for this gene family from the Hymenochaetales. However, since our gene and protein characterization is based on similarities to homologous MnPs and not yet confirmed by cDNA sequences, we present these currently as predicted features only.

Despite the long evolutionary distance between the Hymenochaetales and both the Polyporales and Agaricales, which host the majority of characterized ligninolytic peroxidases, the

deduced *Fomitiporia* protein sequences maintain a set of key characteristics that are highly conserved among fungal peroxidases. Regarding the presence of residues involved in heme pocket formation, Ca<sup>2+</sup> binding, disulfide bond formation and length and predicted mass of the mature proteins, predicted isoelectric points, and substrate binding residues, the characterized *Fomitiporia* sequences adhere to the norm (2). The presence of the manganese-binding residues and the lack of the exposed tryptophan characterize the enzymes best as MnPs. Notably, there are differences compared to well-characterized MnPs. The position of the exposed tryptophan residue characterizing LiPs and VPs is usually occupied by either an alanine or serine residue in MnPs, but in the *Fomitiporia* MnPs this position is occupied by an asparagine (FmMnP1) or a histidine (FmMnP2 and FmMnP3). The only other class II peroxidase with a histidine in this position is from *Trametes cervina* (BAE46585 tclip), an enzyme that has been characterized to perform LiP-like reactions (39). This performance has been attributed to a unique surface-exposed tyrosine residue and received support from homology modeling (38, 55). However, it has also been suggested that the imidazol side group of histidine could serve as a radical stabilizing group in a manner analogous to the indol group of tryptophan (32). This would suggest a new type of VP in the Hymenochaetales, an idea that is further supported by the conservation of this residue in partial sequences of other hymenochaetalean taxa (*Phylloporia ribis*, *Hymenochaete corrugata*, *Phellinidium ferrugineofuscum*) that form a clade with FmMnP2 and FmMnP3. However, site-directed mutagenesis that replaced the catalytic tryptophan with a histidine in a *Pleurotus eryngii* VP did not support an equivalent role for histidine in this position (56). Mechanistic studies to characterize the biochemical properties of *Fomitiporia* peroxidases are urgently needed.

MnPs can be distinguished as long or "classical" MnPs and short MnPs (24, 41). The former contain 10 cysteine residues involved in forming five disulfide bonds, whereas the latter form only four disulfide bonds. Isoforms FmMnP1 and FmMnP2 contain 10 cysteine residues and are predicted to form five disulfide bonds. FmMnP3 is unique among all known full-length class II peroxidases in having two additional cysteine residues that could be involved in forming a sixth disulfide bond. The reduced intron number is a further characteristic that is shared between the *Fomitiporia* sequences and the long MnPs, but in terms of overall length the *Fomitiporia* sequences resemble the short MnPs more. The unique intron arrangement in *Fmmnp* genes could lead to further diversification in this lineage if subjected to alternative or altered splicing. The latter event has been observed in *P. chrysosporium* *lip* and *mnp* genes (61). However, we have no indication of the presence of additional isoforms due to aberrant transcriptional events in these genes.

We examined the expression of three *mnp* genes in *Fomitiporia mediterranea* as a function of mRNA transcript abundance. Transcript abundance can vary as a result of transcriptional activity or differences in mRNA transcript stability among the investigated genes. The expression of *mnp* genes in various basidiomycete species is regulated at the transcriptional level and depends on a sufficient concentration of Mn in the growth medium (7, 27, 49). Optimal Mn concentrations seem to vary among species, but up to 200  $\mu$ M Mn has been

found to favor expression, whereas higher concentrations can have an inhibitory effect (6, 21, 27). Even under optimal culture conditions, MnP activity tends to peak after 5 to 9 days of idiophasic growth (5, 7). Our expression results are in concordance with these findings for two of the three *mnp* genes. Isoform *Fmmnp1* and *Fmmnp2* expression levels reached a maximum at day 5 of growth in high-Mn concentration, nutrient-limited medium. Isoform *Fmmnp3* transcript levels did not depend on Mn concentration, indicating a differential expression of the *mnp* genes in *F. mediterranea*. A similar observation has been made in *P. chrysosporium*, where the *mnp3* gene is expressed in an Mn-independent way (17).

The phylogenetic analyses (Fig. 1) are consistent with our previous findings regarding the evolutionary history of the class II peroxidase family (41). These can be summarized as follows: (i) manganese peroxidases are the most widespread ligninolytic peroxidases, both in terms of taxonomic occurrence and phylogenetic distribution; (ii) VPs have evolved multiple times independently from MnP predecessors; and (iii) LiPs are monophyletic and have evolved just once in the Polyporales from a VP ancestor by losing the manganese-binding site. The addition of more sequences from previously unrepresented taxa adds further insight into the evolutionary history of the gene family. Class II peroxidases of the Hymenochaetales are not monophyletic but belong to two lineages that had separated early in the evolution of the gene family. This split distribution is also observed for sequences from other orders of the Agaricomycotina, e.g., the Polyporales and Agaricales. Presumably, an ancestral form of the Agaricomycotina already harbored multiple peroxidase genes as a result of gene duplication events before the Agaricomycotina split into its major clades.

The rather small assemblage of basal class II peroxidases lacks the residues important for ligninolysis. The only class II sequence in the recently published genome of the brown rot fungus *Postia placenta* belongs to this basal group supporting the notion that ligninolytic peroxidases do not play a role in brown rot decay (36).

Whether ectomycorrhizal taxa harbor ligninolytic peroxidase genes has been an intriguing question. Earlier reports could not be substantiated (10). However, a recent study showed that multiple ECM taxa harbor class II peroxidases closely related to MnPs (4). In our analysis, they cluster with the full-length sequence from *Laccaria bicolor*, which lacks the ligninolytic residues. Although the sequences show a higher affinity to MnPs than the basal sequences, the sister relationship to clade MnP1 shown in Fig. 1 is not strongly supported. The only ectomycorrhizal sequence that is placed with strong support within one of the ligninolytic groups is the partial sequence from *Gomphus clavatus* nested in clade MnP1. Our analysis suggests that this species would be a suitable candidate for further studies directed at solving the question regarding the presence of ligninolytic peroxidases in ECM fungi.

Manganese peroxidases are clearly polyphyletic. The majority of the sequences fall into one strongly supported (96/1.0) clade (Fig. 1, MnP1). The remaining groups containing MnPs (MnP2 to MnP4) are not supported as being monophyletic and are intermixed with VPs. This indicates that switches from an MnP to a VP, presumably due to a single point mutation, are not only possible but may have occurred multiple times. How-



ever, no indication of a reversal from a VP to an MnP can be drawn from the phylogenetic analysis.

Among white rot fungal taxa, *P. cinnabarinus* has been considered an exception because it has been reported to secrete only laccases as lignin-degrading enzymes and not peroxidases (13). Our successful amplification of peroxidase sequences and the phylogenetic analysis suggests that this fungus harbors at least three *lip* genes and two *mnp* genes. In light of these findings, there is no evidence that white rot lignin degradation is possible without any of the ligninolytic peroxidases. The sequences from the two strains we used are either identical or differ only in a single aa position. It remains to be resolved why peroxidase activity under ligninolytic conditions for *P. cinnabarinus* is not readily demonstrable. One possibility is that these genes are differentially regulated and are not secreted under common laboratory conditions. An alternative explanation is that the genes are expressed but not freely secreted in the surrounding medium, instead remaining attached to a sheet surrounding the fungal hyphae. A similar discrepancy between enzymatic activity and putative gene content has been observed for *Phanerochaete sordida* and *Ceriporiopsis subvermispora*, which lack LiP activity but seem to have *lip* genes (50, 57, 58).

#### ACKNOWLEDGMENTS

This research was supported in part by National Science Foundation award DEB-0732968 to D.S.H.

The culture of *F. mediterranea* MF3/22 was provided as a gift by Michael Fischer. We are thankful to Inga Bødeker for providing us with class II sequence information from ectomycorrhizal taxa.

#### REFERENCES

- Balan, D. S., and R. T. Monteiro. 2001. Decolorization of textile indigo dye by ligninolytic fungi. *J. Biotechnol.* **89**:141–145.
- Banci, L. 1997. Structural properties of peroxidases. *J. Biotechnol.* **53**:253–263.
- Bendtsen, J. D., H. Nielsen, G. von Heijne, and S. Brunak. 2004. Improved prediction of signal peptides: SignalP 3.0. *J. Mol. Biol.* **340**:783–795.
- Bødeker, I. T., C. M. Nygren, A. F. Taylor, A. Olson, and B. D. Lindahl. 2009. Class II peroxidase-encoding genes are present in a phylogenetically wide range of ectomycorrhizal fungi. *ISME J.* **3**:1387–1395.
- Bogan, B. W., B. Schoenike, R. T. Lamar, and D. Cullen. 1996. Manganese peroxidase mRNA and enzyme activity levels during bioremediation of polycyclic aromatic hydrocarbon-contaminated soil with *Phanerochaete chrysosporium*. *Appl. Environ. Microbiol.* **62**:2381–2386.
- Bonnarme, P., and T. W. Jeffries. 1990. Mn(II) regulation of lignin peroxidases and manganese-dependent peroxidases from lignin-degrading white rot fungi. *Appl. Environ. Microbiol.* **56**:210–217.
- Brown, J. A., J. K. Glenn, and M. H. Gold. 1990. Manganese regulates expression of manganese peroxidase by *Phanerochaete chrysosporium*. *J. Bacteriol.* **172**:3125–3130.
- Brown, J. A., D. Li, M. Alic, and M. H. Gold. 1993. Heat shock induction of manganese peroxidase gene transcription in *Phanerochaete chrysosporium*. *Appl. Environ. Microbiol.* **59**:4295–4299.
- Camarero, S., S. Sarkar, F. J. Ruiz-Dueñas, M. J. Martínez, and A. T. Martínez. 1999. Description of a versatile peroxidase involved in the natural degradation of lignin that has both manganese peroxidase and lignin peroxidase substrate interaction sites. *J. Biol. Chem.* **274**:10324–10330.
- Chen, D. M., A. F. S. Taylor, R. M. Burke, and J. W. G. Cairney. 2001. Identification of genes for lignin peroxidases and manganese peroxidases in ectomycorrhizal fungi. *New Phytologist* **152**:151–158.
- Del Rio, J. A., P. Gomez, A. Baidez, M. D. Fuster, A. Ortuno, and V. Frias. 2004. Phenolic compounds have a role in the defence mechanism protecting grapevine against fungi involved in Petri disease. *Phytopathologia Mediterranea* **43**:87–94.
- Doyle, W. A., W. Blodig, N. C. Veitch, K. Piontek, and A. T. Smith. 1998. Two substrate interaction sites in lignin peroxidase revealed by site-directed mutagenesis. *Biochemistry* **37**:15097–15105.
- Eggert, C., U. Temp, and K. E. Eriksson. 1996. The ligninolytic system of the white rot fungus *Pycnoporus cinnabarinus*: purification and characterization of the laccase. *Appl. Environ. Microbiol.* **62**:1151–1158.
- Elena, K., M. Fischer, D. Dimou, and D. M. Dimou. 2006. *Fomitiporia mediterranea* infecting citrus trees in Greece. *Phytopathologia Mediterranea* **45**:35–39.
- Fischer, M. 2002. A new wood-decaying basidiomycete species associated with esca of grapevine: *Fomitiporia mediterranea* (Hymenochaetales). *Mycol. Prog.* **1**:315–324.
- Fischer, M. 2006. Biodiversity and geographic distribution of basidiomycetes causing esca-associated white rot in grapevine: a worldwide perspective. *Phytopathologia Mediterranea* **45**:S30–S42.
- Gettemy, J. M., B. Ma, M. Alic, and M. H. Gold. 1998. Reverse transcription-PCR analysis of the regulation of the manganese peroxidase gene family. *Appl. Environ. Microbiol.* **64**:569–574.
- Glenn, J. K., L. Akileswaran, and M. H. Gold. 1986. Mn(II) oxidation is the principal function of the extracellular Mn-peroxidase from *Phanerochaete chrysosporium*. *Arch. Biochem. Biophys.* **251**:688–696.
- Glenn, J. K., and M. H. Gold. 1985. Purification and characterization of an extracellular Mn(II)-dependent peroxidase from the lignin-degrading basidiomycete, *Phanerochaete chrysosporium*. *Arch. Biochem. Biophys.* **242**:329–341.
- Glenn, J. K., M. A. Morgan, M. B. Mayfield, M. Kuwahara, and M. H. Gold. 1983. An extracellular H<sub>2</sub>O<sub>2</sub>-requiring enzyme preparation involved in lignin biodegradation by the white rot basidiomycete *Phanerochaete chrysosporium*. *Biochem. Biophys. Res. Commun.* **114**:1077–1083.
- Hakala, T. K., K. Hilden, P. Majjala, C. Olsson, and A. Hatakka. 2006. Differential regulation of manganese peroxidases and characterization of two variable MnP encoding genes in the white-rot fungus *Physisporinus rivulosus*. *Appl. Microbiol. Biotechnol.* **73**:839–849.
- Hammel, K. E., and D. Cullen. 2008. Role of fungal peroxidases in biological ligninolysis. *Curr. Opin. Plant Biol.* **11**:349–355.
- Hibbett, D. S. 2006. A phylogenetic overview of the Agaricomycotina. *Mycologia* **98**:917–925.
- Hildén, K., A. T. Martínez, A. Hatakka, and T. Lundell. 2005. The two manganese peroxidases Pr-MnP2 and Pr-MnP3 of *Phlebia radiata*, a lignin-degrading basidiomycete, are phylogenetically and structurally divergent. *Fungal Genet. Biol.* **42**:403–419.
- Huang, S. T., S. S. Tzean, B. Y. Tsai, and H. J. Hsieh. 2009. Cloning and heterologous expression of a novel ligninolytic peroxidase gene from poroid brown-rot fungus *Antrodia cinnamomea*. *Microbiology* **155**:424–433.
- Huelsbeck, J. P., and F. Ronquist. 2001. MRBAYES: Bayesian inference of phylogenetic trees. *Bioinformatics* **17**:754–755.
- Johansson, T., P. O. Nyman, and D. Cullen. 2002. Differential regulation of *mnp2*, a new manganese peroxidase-encoding gene from the ligninolytic fungus *Trametes versicolor* PRL 572. *Appl. Environ. Microbiol.* **68**:2077–2080.
- Katoh, K., K. Kuma, H. Toh, and T. Miyata. 2005. MAFFT version 5: improvement in accuracy of multiple sequence alignment. *Nucleic Acids Res.* **33**:511–518.
- Katoh, K., K. Misawa, K. Kuma, and T. Miyata. 2002. MAFFT: a novel method for rapid multiple sequence alignment based on fast Fourier transform. *Nucleic Acids Res.* **30**:3059–3066.
- Kirk, T. K., E. Schultz, W. J. Connors, L. F. Lorenz, and J. G. Zeikus. 1978. Influence of culture parameters on lignin metabolism by *Phanerochaete chrysosporium*. *Arch. Microbiol.* **117**:277–285.
- Larsson, K. H., E. Parmasto, M. Fischer, E. Langer, K. K. Nakasone, and S. A. Redhead. 2006. Hymenochaetales: a molecular phylogeny for the hymenochaetoid clade. *Mycologia* **98**:926–936.
- Lassmann, G., L. A. Eriksson, F. Himo, F. Lenzian, and W. Lubitz. 1999. Electronic structure of a transient histidine radical in liquid aqueous solution: EPR continuous-flow studies and density functional calculations. *J. Phys. Chem. A* **103**:1083–1290.
- Li, D., M. Alic, J. A. Brown, and M. H. Gold. 1995. Regulation of manganese peroxidase gene transcription by hydrogen peroxide, chemical stress, and molecular oxygen. *Appl. Environ. Microbiol.* **61**:341–345.
- Li, D., M. Alic, and M. H. Gold. 1994. Nitrogen regulation of lignin peroxidase gene transcription. *Appl. Environ. Microbiol.* **60**:3447–3449.
- Martin, F., A. Aerts, D. Ahren, A. Brun, E. G. Danchin, F. Duchaussoy, J. Gibon, A. Kohler, E. Lindquist, V. Pereda, A. Salamov, H. J. Shapiro, J. Wuyts, D. Blaudez, M. Buee, P. Brokstein, B. Canback, D. Cohen, P. E. Courty, P. M. Coutinho, C. Delaruelle, J. C. Detter, A. Deveau, S. DiFazio, S. Duplessis, L. Fraissinet-Tachet, E. Lucic, P. Frey-Klett, C. Fourrey, I. Feussner, G. Gay, J. Grimwood, P. J. Hoegger, P. Jain, S. Kilaru, J. Labbe, Y. C. Lin, V. Legue, F. Le Tacon, R. Marmeisse, D. Melayah, B. Montanini, M. Muratet, U. Nehls, H. Niculita-Hirzel, M. P. Oudot-Le Secq, M. Peter, H. Quesneville, B. Rajashekar, M. Reich, N. Rouhier, J. Schmutz, T. Yin, M. Chalot, B. Henrissat, U. Kues, S. Lucas, Y. Van de Peer, G. K. Podila, A. Polle, P. J. Pukkila, P. M. Richardson, P. Rouze, I. R. Sanders, J. E. Stajich, A. Tunlid, G. Tuskan, and I. V. Grigoriev. 2008. The genome of *Laccaria bicolor* provides insights into mycorrhizal symbiosis. *Nature* **452**:88–92.
- Martinez, D., J. Challacombe, I. Morgenstern, D. Hibbett, M. Schmöll, C. P. Kubicek, P. Ferreira, F. J. Ruiz-Duenas, A. T. Martinez, P. Kersten, K. E. Hammel, A. Vanden Wymelenberg, J. Gaskell, E. Lindquist, G. Sabat, S. S. Bondurant, L. F. Larrondo, P. Canessa, R. Vicuna, J. Yadav, H. Doddappa

- neni, V. Subramanian, A. G. Pisabarro, J. L. Lavin, J. A. Oguiza, E. Master, B. Henrissat, P. M. Coutinho, P. Harris, J. K. Magnuson, S. E. Baker, K. Bruno, W. Kenealy, P. J. Hoegger, U. Kues, P. Ramaiya, S. Lucas, A. Salamov, H. Shapiro, H. Tu, C. L. Chee, M. Misra, G. Xie, S. Teter, D. Yaver, T. James, M. Mokrejs, M. Pospisek, I. V. Grigoriev, T. Brettin, D. Rokhsar, R. Berka, and D. Cullen. 2009. Genome, transcriptome, and secretome analysis of wood decay fungus *Postia placenta* supports unique mechanisms of lignocellulose conversion. *Proc. Natl. Acad. Sci. U. S. A.* **106**:1954–1959.
37. Mester, T., K. Ambert-Balay, S. Ciofi-Baffoni, L. Banci, A. D. Jones, and M. Tien. 2001. Oxidation of a tetrameric nonphenolic lignin model compound by lignin peroxidase. *J. Biol. Chem.* **276**:22985–22990.
38. Miki, Y., H. Ichinose, and H. Wariishi. 2010. Molecular characterization of lignin peroxidase from the white-rot basidiomycete *Trametes cervina*: a novel fungal peroxidase. *FEMS Microbiol. Lett.* **304**:39–46.
39. Miki, Y., H. Tanaka, M. Nakamura, and H. Wariishi. 2006. Isolation and characterization of a novel lignin peroxidase from the white-rot basidiomycete *Trametes cervina*. *J. Fac. Agr. Kyushu Univ.* **51**:99–104.
40. Moen, M. A., and K. E. Hammel. 1994. Lipid peroxidation by the manganese peroxidase of *Phanerochaete chrysosporium* is the basis for phenanthrene oxidation by the intact fungus. *Appl. Environ. Microbiol.* **60**:1956–1961.
41. Morgenstern, I., S. Klopman, and D. S. Hibbett. 2008. Molecular evolution and diversity of lignin degrading heme peroxidases in the Agaricomycetes. *J. Mol. Evol.* **66**:243–257.
42. Mugnai, L., A. Graniti, and G. Surico. 2007. Esca (black measles) and brown wood-streaking: two old and elusive diseases of grapevines. *Plant Dis.* **83**:404–418.
43. Mugnai, L., G. Surico, and A. Sfalanga. 1997. Produzione di enzimi esocellulari da parte di funghi del legno di viti colpite dal 'mal dell'esca'. *Micologia Italiana* **26**:11–22.
44. Muller, P. Y., H. Janovjak, A. R. Miserez, and Z. Dobbie. 2002. Processing of gene expression data generated by quantitative real-time RT-PCR. *Biotechniques* **32**:1372–1374, 1376, 1378–1379.
45. Novotný, C., B. Rawal, M. Bhatt, M. Patel, V. Sasek, and H. P. Molitoris. 2001. Capacity of *Irpex lacteus* and *Pleurotus ostreatus* for decolorization of chemically different dyes. *J. Biotechnol.* **89**:113–122.
46. Overton, B. E., E. L. Stewart, and N. G. Wenner. 2006. Manganese oxidation in Petri disease fungi as a novel taxonomic character. *Phytopathologia Mediterranea* **45**:S131–S134.
47. Passardi, F., N. Bakalovic, F. K. Teixeira, M. Margis-Pinheiro, C. Penel, and C. Dunand. 2007. Prokaryotic origins of the non-animal peroxidase superfamily and organelle-mediated transmission to eukaryotes. *Genomics* **89**:567–579.
48. Pérez-Boada, M., F. J. Ruiz-Dueñas, R. Pogni, R. Basosi, T. Choinowski, M. J. Martínez, K. Piontek, and A. T. Martínez. 2005. Versatile peroxidase oxidation of high redox potential aromatic compounds: site-directed mutagenesis, spectroscopic and crystallographic investigation of three long-range electron transfer pathways. *J. Mol. Biol.* **354**:385–402.
49. Périć, F. H., and M. H. Gold. 1991. Manganese regulation of manganese peroxidase expression and lignin degradation by the white rot fungus *Dichomitus squalens*. *Appl. Environ. Microbiol.* **57**:2240–2245.
50. Rajakumar, S., J. Gaskell, D. Cullen, S. Lobos, E. Karahanian, and R. Vicuna. 1996. Lip-like genes in *Phanerochaete sordida* and *Ceriporiopsis subvermisporea*, white rot fungi with no detectable lignin peroxidase activity. *Appl. Environ. Microbiol.* **62**:2660–2663.
51. Romanazzi, G., S. Murolo, L. Pizzichini, and S. Nardi. 2009. Esca in young and mature vineyards, and molecular diagnosis of the associated fungi. *Eur. J. Plant Pathol.* **125**:277–290.
52. Ronquist, F., and J. P. Huelsenbeck. 2003. MrBayes 3: Bayesian phylogenetic inference under mixed models. *Bioinformatics* **19**:1572–1574.
53. Ruiz-Dueñas, F. J., F. Guillén, S. Camarero, M. Pérez-Boada, M. J. Martínez, and A. T. Martínez. 1999. Regulation of peroxidase transcript levels in liquid cultures of the ligninolytic fungus *Pleurotus eryngii*. *Appl. Environ. Microbiol.* **65**:4458–4463.
54. Ruiz-Dueñas, F. J., and A. T. Martínez. 2009. Microbial degradation of lignin: how a bulky recalcitrant polymer is efficiently recycled in nature and how we can take advantage of this. *Microb. Biotechnol.* **2**:164–177.
55. Ruiz-Dueñas, F. J., M. Morales, E. García, Y. Miki, M. J. Martínez, and A. T. Martínez. 2009. Substrate oxidation sites in versatile peroxidase and other basidiomycete peroxidases. *J. Exp. Bot.* **60**:441–452.
56. Ruiz-Dueñas, F. J., R. Pogni, M. Morales, S. Giansanti, M. J. Mate, A. Romero, M. J. Martínez, R. Basosi, and A. T. Martínez. 2009. Protein radicals in fungal versatile peroxidase: catalytic tryptophan radical in both compound I and compound II and studies on W164Y, W164H, and W164S variants. *J. Biol. Chem.* **284**:7986–7994.
57. Rüttimann-Johnson, C., D. Cullen, and R. T. Lamar. 1994. Manganese peroxidases of the white rot fungus *Phanerochaete sordida*. *Appl. Environ. Microbiol.* **60**:599–605.
58. Rüttimann-Johnson, C., L. Salas, R. Vicuna, and T. K. Kirk. 1993. Extracellular enzyme production and synthetic lignin mineralization by *Ceriporiopsis subvermisporea*. *Appl. Environ. Microbiol.* **59**:1792–1797.
59. Stamatakis, A. 2006. RAxML-VI-HPC: maximum likelihood-based phylogenetic analyses with thousands of taxa and mixed models. *Bioinformatics* **22**:2688–2690.
60. Stewart, P., P. Kersten, A. Vanden Wymelenberg, J. Gaskell, and D. Cullen. 1992. Lignin peroxidase gene family of *Phanerochaete chrysosporium*: complex regulation by carbon and nitrogen limitation and identification of a second dimorphic chromosome. *J. Bacteriol.* **174**:5036–5042.
61. Stuardo, M., F. Larrondo Luis, M. Vásquez, R. Vicuña, and B. González. 2005. Incomplete processing of peroxidase transcripts in the lignin degrading fungus *Phanerochaete chrysosporium*. *FEMS Microbiol. Lett.* **242**:37–44.
62. Sundaramoorthy, M., K. Kishi, M. H. Gold, and T. L. Poulos. 1994. The crystal structure of manganese peroxidase from *Phanerochaete chrysosporium* at 2.06-Å resolution. *J. Biol. Chem.* **269**:32759–32767.
63. Surico, G., L. Mugnai, and G. Marchi. 2008. The esca disease complex, p. 119–136. *In* A. Ciancio and K. G. Mukerji (ed.), *Integrated management of diseases caused by fungi, phytoplasma and bacteria*. Springer, New York, NY.
64. Tedersoo, L., T. W. May, and M. E. Smith. 2010. Ectomycorrhizal lifestyle in Fungi: global diversity, distribution and evolution of phylogenetic lineages. *Mycorrhiza* **20**:217–263.
65. Tien, M., and K. Kirk. 1983. Lignin-degrading enzyme from the hymenomycete *Phanerochaete chrysosporium*. *Science* **221**:661–663.
66. Wariishi, H., K. Valli, and M. H. Gold. 1992. Manganese(II) oxidation by manganese peroxidase from the basidiomycete *Phanerochaete chrysosporium*. Kinetic mechanism and role of chelators. *J. Biol. Chem.* **267**:23688–23695.
67. Welinder, K. G. 1992. Superfamily of plant, fungal and bacterial peroxidases. *Curr. Opin. Struct. Biol.* **2**:388–393.